J. Fluid Mech. (1978), *vol.* 90, *part* 3, *pp.* 433–447
Printed in Great Britain

Laminar flow in the entrance region of a smooth pipe

By A. K. MOHANTY AND S. B. L. ASTHANA
Department of Mechanical Engineering, Indian Institute of Technology, Kharagpur

(Received 22 December 1977 and in revised form 14 June 1978)

The entrance region has been divided into two parts, the inlet region and the filled region. At the end of the inlet region, the boundary layers meet at the pipe axis but the velocity profiles are not yet similar. In the filled region, adjustment of the completely viscous profile takes place until the Poiseuille similar profile is attained at the end of it. The boundary-layer equations in the inlet region and the Navier–Stokes equations with order-of-magnitude analysis in the filled region are solved using fourth-degree velocity profiles. The total length of the entrance region so obtained is $\xi = x/R\,Re = 0{\cdot}150$, whereas the boundary layers are observed to meet at approximately one-quarter of the entrance length, i.e. at $\xi = 0{\cdot}036$. Experiments reported in the paper corroborate the analytical results.

1. Introduction

Investigation of fluid flow in the entrance region of a pipe or a duct is of considerable practical significance and, not surprisingly, there exist a large number of references in the literature on this topic, especially for incompressible laminar flow. Historically, the person first to analyse the entrance flow through a smooth pipe was Schiller (1922; see Schlichting 1968, p. 231), who used integral analysis of a parabolic velocity profile in the boundary layer. The velocity profile chosen was a modification of the Poiseuille solution in the sense that the pipe radius was replaced by the boundary-layer thickness. In other words, when the boundary-layer thickness δ became equal to the pipe radius R, the analysis predicted automatic establishment of fully developed flow. This apparently gave rise to the idea that the attainment of a fully developed profile is synonymous with δ being equal to R, a notion which has been regarded as suspect qualitatively (Goldstein 1938, p. 299; Rosenhead 1963, p. 440). Schiller's integral solution on the basis of a parabolic profile is inherently questionable, as such a profile does not ensure attainment of free-stream conditions at the edge of the boundary layer by not permitting the second derivative of the velocity to be zero, which is an essential boundary condition for flow with a pressure gradient.

Later studies, such as that of Schlichting (1968, p. 176), have been primarily oriented towards the investigation of the development of the velocity profile. Schlichting's procedure for a rectangular duct consists of matching a downstream boundary-layer solution with a velocity profile which deviates increasingly from the Poiseuille profile in the upstream direction. This method of perturbing a Poiseuille profile was first adopted by Boussinesq (1891; see Van Dyke 1970). The matching is supposed to take place where the boundary-layer and the deformed-profile solutions are valid simultaneously. This procedure of Schlichting has been re-examined by Van Dyke (1970) and Wilson (1971), whose major corrections to Schlichting's method

consist of proposing second-order stream functions to account for the displacement thickness in the boundary-layer region.

In general four different methods have been applied to solve the entrance flow. Van Dyke (1970) lists these methods as (i) numerical finite-difference solution of the boundary-layer equations, (ii) linearization of the inertia terms, (iii) integral methods and (iv) series expansion, and comments on the assumptions common to the last two methods in so far as accounting for the displacement thickness is concerned. Fargie & Martin (1971), on the other hand, give a relatively exhaustive review, including classification of the most important work by these different methods. More recently Sparrow & Anderson (1977) have considered the effects of the inlet profile on the development length in a parallel-plate channel by treating the flow fields upstream and downstream of the entry simultaneously.

In such analysis, for example that by Schlichting, though the entrance region has been tacitly divided into two parts, no quantitative value seems to have been indicated for the distance at which the boundary layers meet at the duct axis. Furthermore, the recommendations of Van Dyke and Wilson have not been applied to axisymmetric pipe flow. In practice, one often comes across flow in a short pipe, such as a pipe leading to a diffuser, a nozzle or a connecting piece, where a knowledge of the development of the boundary-layer thickness is of considerable importance.

In a recent experimental investigation wherein velocity profiles in various potential and viscous zones at the entrance to a diffuser were created by passing the flow through pipes of various length-to-diameter ratios, the present authors found that the laminar boundary layers meet at the pipe axis much earlier than the attainment of a fully developed profile. The existing literature did not seem to indicate quantitatively the location of such a meeting of the boundary layers.

This observation motivated the present authors to re-examine analytically the flow in the pipe entrance, and verify salient results by experiments.

2. Physical model

In this paper, an analysis is presented to estimate for a smooth circular pipe the growth of the boundary layer under the accelerating core, and the subsequent adjustment of the completely viscous velocity profile to the Poiseuille solution marking the end of the entrance region. For convenience the boundary-layer region is identified as the 'inlet region' and the fully viscous region as the 'filled region', after Shingo (1966). The physical model is illustrated in figure 1.

The existence of the inlet and the filled regions was verified experimentally at Reynolds numbers of 1875, 2500 and 3250.

3. Governing equations

Boundary-layer equations are valid in the inlet region while the full Navier–Stokes equations have to be applied to the flow in the filled region. However, since the length of the filled region was found experimentally by the present authors to be very large compared with the pipe radius, in contrast to White's (1974) implication of a short length, order-of-magnitude analysis of the Navier–Stokes equations is considered permissible. It is observed that in such an analysis the equations in the filled region are

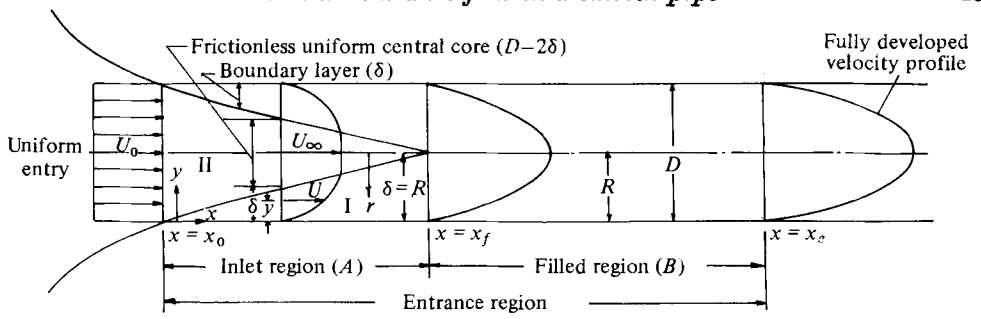

FIGURE 1. Physical model of entrance region.

similar in form to those in the boundary layer, although the 'free-stream' (pipe centre) conditions in the two regions differ.

Apart from the inclusion of the filled region, the present analysis, which uses integral methods, has the following aims.

(i) To ensure smoother attainment of the free-stream condition by requiring the second derivative of the velocity profile at the edge of the boundary layer to be zero, unlike the case of Schiller. The prediction of too low an entrance length by McComas (1967), which has been attributed by Fargie & Martin (1971) to omission of viscous effects, resulted from a Schiller-like choice of the velocity profile.

(ii) To account for the viscous effects on mass flow by considering the area-averaged continuity equation at a section in terms of the displacement thickness, and then solving the differentiated displacement-thickness equation simultaneously with the momentum equation.

(iii) To refer the development length to the average velocity rather than to the centre-line value since, with the introduction of the filled region, the centre-line velocity cannot be assessed independently, say by Bernoulli's equation, as in a pure boundary layer model.

With the origin of the co-ordinate system located at the pipe centre at the inlet, the appropriate conservation equations are

$$\partial(ru)/\partial x + \partial(rv)/\partial r = 0 \quad \text{(mass)}, \tag{1}$$

$$\left.\begin{aligned} u\frac{\partial u}{\partial x} + v\frac{\partial u}{\partial r} &= -\frac{1}{\rho}\frac{\partial p}{\partial x} + \frac{\nu}{r}\frac{\partial}{\partial r}\left(r\frac{\partial u}{\partial r}\right) \\ \partial p/\partial r &= 0 \end{aligned}\right\} \quad \text{(momentum)}. \tag{2}$$

The boundary conditions are as follows:

(*a*) *Inlet region*

(i) $u = v = 0$ at $r = R$ (no slip at the wall).

(ii) $u = U_\infty(x)$, (iii) $\partial u/\partial r = 0$ } for $0 \leqslant r \leqslant R-\delta$ (free stream),

where $U_\infty(x)$ is the local potential core velocity.

(iv) $\partial^2 u/\partial r^2 = 0$ at $0 \leqslant r \leqslant R-\delta$,

to ensure an accurate approach to the free stream in the presence of a pressure gradient.

(v) $$\left[\frac{\nu}{r}\frac{\partial}{\partial r}\left(r\frac{\partial u}{\partial r}\right)\right]_{r=R} = \frac{1}{\rho}\frac{\partial p}{\partial x},$$

which is the reduced form of the boundary-layer equation at the wall. Using Bernoulli's equation for flow in the potential core, condition (v) is modified to

$$\nu\left[\frac{\partial^2 u}{\partial r^2}\right]_{r=R}+\left[\frac{\nu}{R}\frac{\partial u}{\partial r}\right]_{r=R}=-U_\infty\frac{dU_\infty}{dx}. \tag{3}$$

(*b*) *Filled region*

(i) $u = v = 0$ at $r = R$ (no slip at the wall).

(ii) $\partial u/\partial r = 0$ at $r = 0$ (condition of symmetry of the velocity profile).

(iii) At the pipe axis, though there is no potential core, the flow is assumed parallel and the velocity there is defined as U_c. Thus the momentum equation at $r = 0$ is

$$U_c\frac{dU_c}{dx}=-\frac{1}{\rho}\frac{dp}{dx}+\left[\frac{\nu}{r}\frac{\partial}{\partial r}\left(r\frac{\partial u}{\partial r}\right)\right]_{r=0}.$$

Pohlhausen's pressure-gradient parameter is defined as

$$\lambda=\begin{cases}\dfrac{\delta^2}{\nu}\dfrac{dU_\infty}{dx} & \text{in the inlet region,}\\[2ex] \dfrac{R^2}{\nu}\dfrac{dU_c}{dx} & \text{in the filled region.}\end{cases} \tag{4}$$

An additional parameter (cf. Shingo 1966) is defined for the filled region as

$$\Gamma=\frac{R^2}{U_c}\left[\frac{\partial^2 u}{\partial r^2}\right]_{r=0}. \tag{5}$$

By expanding in a Taylor series, it is noted that

$$\left[\frac{1}{r}\frac{\partial}{\partial r}\left(r\frac{\partial u}{\partial r}\right)\right]_{r=0}=2\left[\frac{\partial^2 u}{\partial r^2}\right]_{r=0},$$

and use of the definitions of λ and Γ makes it possible to write the pressure-gradient term in boundary condition (iii) for the filled region as

$$-\frac{R^2}{\mu U_c}\frac{dp}{dx}=\lambda-2\Gamma. \tag{6}$$

The pressure gradient in the inlet region can be expressed in a similar manner as

$$-\frac{\delta^2}{\mu U_\infty}\frac{dp}{dx}=\lambda. \tag{7}$$

3.1. *Integral form of the governing equations*

The boundary-layer equations in the inlet region are integrated according to the von Kármán–Pohlhausen scheme. The (x, r) co-ordinate system is first changed to an (x, y) system, as shown in figure 1.

As stated earlier, the reduced equations in the filled region are also of boundary-layer type; hence a similar integration is carried out between the limits $y = 0$ and $y = R$, in contrast to $y = 0$ and $y = \delta(x)$ in the inlet region.

In order to convey the generality of the integrated form of the conservation equations, we shall let $\delta(x)$, U_c and Γ, respectively, be equal to R in the filled region and take $U_\infty \equiv U_c$, and $\Gamma = 0$ in the inlet region.

The transverse velocity component v is easily evaluated from the continuity equation, and is substituted into the momentum equation, which when integrated has the form

$$R\frac{\partial}{\partial x}\left[U_\infty^2\int_0^\delta \frac{u}{U_\infty}\left(1-\frac{u}{U_\infty}\right)\left(1-\frac{y}{R}\right)dy\right]+RU_\infty\frac{dU_\infty}{dx}\int_0^\delta\left(1-\frac{u}{U_\infty}\right)\left(1-\frac{y}{R}\right)dy$$
$$-R^2\nu\left[\frac{\partial^2 u}{\partial y^2}\right]_{y=\delta}-\nu R\left[\frac{\partial u}{\partial y}\right]_{y=0}=0. \tag{8}$$

Note that, although $[\partial^2 u/\partial y^2]_{y=\delta}$ can be taken as zero in the inlet region, its value is *a priori* unknown in the filled region.

We now define the displacement and momentum thicknesses as

$$\delta^* = \int_0^\delta\left(1-\frac{u}{U_\infty}\right)\left(1-\frac{y}{R}\right)dy,$$

$$\delta^{**} = \int_0^\delta\frac{u}{U_\infty}\left(1-\frac{u}{U_\infty}\right)\left(1-\frac{y}{R}\right)dy,$$

and rewrite (8) as

$$\frac{d\delta^{**}}{dx}+(2\delta^{**}+\delta^*)\frac{1}{U_\infty}\frac{dU_\infty}{dx}-\frac{R\nu}{U_\infty^2}\left[\frac{\partial^2 u}{\partial y^2}\right]_{y=\delta}-\frac{\nu}{U_\infty^2}\left[\frac{\partial u}{\partial y}\right]_{y=0}=0. \tag{9}$$

Use of the definitions of the pressure-gradient parameters and skin-friction coefficient allows (9) to be written in the form

$$\frac{d\delta^{**}}{dx}+(2\delta^{**}+\delta^*)\frac{\nu\lambda}{\delta^2 U_c}-\frac{\nu}{R}\frac{\Gamma}{U_c}=\frac{C_f}{2}, \tag{10}$$

where $C_f = \tau_w/\frac{1}{2}\rho U_c^2$. Note that in (10) we have written U_c in place of U_∞ only to convey the generalization. In its present form, (10) applies to the filled region, where the limits of integration for δ^* and δ^{**} are R in lieu of $\delta(x)$, and $U_\infty \equiv U_c$. For the inlet region (10) would have $\Gamma = 0$ and $U_c \equiv U_\infty$.

The conservation of mass is expressed in terms of the displacement thickness by

$$2\pi R U_\infty \delta^* = \pi R^2(U_\infty - U_0),$$

which leads to

$$U_0/U_\infty = 1-2\delta^*/R, \tag{11}$$

where U_0 is the average velocity. We shall use (11) to evaluate the correspondence between the average and core velocities.

In order to solve (10), it is necessary to assume a suitable velocity profile in the boundary layer of the inlet region ($\lambda \neq 0$, $\Gamma = 0$) and a totally viscous profile in the filled region ($\lambda \neq 0$, $\Gamma \neq 0$). The independent variable y and the dependent variable $u(x, y)$ are non-dimensionalized as

$$\eta = \begin{cases} y/\delta & \text{in the inlet region,} \\ y/R & \text{in the filled region,} \end{cases}$$

$$\bar{u} = u(x, y)/U_c(x).$$

In all cases $U_c(x)$ should be replaced by $U_\infty(x)$ in the inlet region.

To account for the pressure gradient in both the inlet and the filled region, a fourth-degree profile whose general form is

$$\bar{u} = \sum_{k=0}^{4} A_k(\lambda, \Gamma)\,\eta^k \tag{12}$$

is assumed in each region.

The five boundary conditions already stated are expressed in the new variables η and $\bar{u}$ as follows.

(*a*) *Inlet region*

(i) $$\bar{u} = \bar{v} = 0 \quad \text{at} \quad \eta = 0. \tag{13a}$$

(ii) $$u = U_\infty(x) \quad \text{or} \quad \bar{u} = 1 \quad \text{at} \quad \eta = 1. \tag{13b}$$

(iii) $$\partial\bar{u}/\partial\eta = 0 \quad \text{at} \quad \eta = 1. \tag{13c}$$

(iv) $$\partial^2 u/\partial\eta^2 = 0 \quad \text{at} \quad \eta = 1. \tag{13d}$$

(v) $$\left[\frac{\partial^2 u}{\partial\eta^2}\right]_{\eta=0} - \frac{\delta}{R}\left[\frac{\partial\bar{u}}{\partial\eta}\right]_{\eta=0} = \lambda. \tag{13e}$$

(*b*) *Filled region*

(i) $$\bar{u} = \bar{v} = 0 \quad \text{at} \quad \eta = 0. \tag{14a}$$

(ii) $$\bar{u} = 1 \quad \text{at} \quad \eta = 1. \tag{14b}$$

(iii) $$\partial\bar{u}/\partial\eta = 0 \quad \text{at} \quad \eta = 1. \tag{14c}$$

(iv) $$\partial^2\bar{u}/\partial\eta^2 = \Gamma \quad \text{at} \quad \eta = 1. \tag{14d}$$

(v) $$\left[\frac{\partial^2\bar{u}}{\partial\eta^2}\right]_{\eta=0} - \left[\frac{\partial\bar{u}}{\partial\eta}\right]_{\eta=0} = 2\Gamma - \lambda. \tag{14e}$$

These boundary conditions on (11) and (12) are satisfied by a velocity profile of the form

$$\bar{u} = F(\eta) + \lambda_1 G(\eta) - \Gamma_1 K(\eta), \tag{15}$$

where

$$\left.\begin{aligned} F(\eta) &= 2\eta - 2\eta^3 + \eta^4, \\ G(\eta) &= \tfrac{1}{6}(\eta - 3\eta^2 + 3\eta^3 - \eta^4), \\ K(\eta) &= (\eta - \tfrac{13}{2}\eta^2 + 10\eta^3 - \tfrac{9}{2}\eta^4), \end{aligned}\right\} \tag{16}$$

$$\lambda_1 = 6(\lambda - 2\delta_1)/(6+\delta_1), \quad \Gamma_1 = \Gamma/(6+\delta_1), \quad \delta_1 = \delta/R.$$

$\delta_1 = 1$ in the filled region; hence $\Gamma_1 = \frac{1}{7}\Gamma$ there. Γ_1 is zero in the inlet region and the resulting profile is the same as that of Pohlhausen.

It should be noted that for the $\lambda_1 = -\frac{12}{7}$ and $\Gamma_1 = -\frac{2}{7}$ the velocity profile reduces to the simple parabolic form

$$\bar{u} = 2\eta - \eta^2 \tag{17}$$

of fully developed incompressible flow. This signifies that the far-downstream asymptotic values (fully developed) of λ_1 and Γ_1 are $-\frac{12}{7}$ and $-\frac{2}{7}$, respectively.

The displacement and momentum thicknesses, using the polynomial (15), are obtained as

$$\frac{\delta^*}{R} = \delta_1^* = \delta_1\left(\frac{3}{10} - \frac{\lambda_1}{120}\right) - \delta_1^2\left(\frac{1}{15} - \frac{\lambda_1}{360}\right) - \frac{\Gamma_1}{40} \tag{18}$$

and

$$\frac{\delta^{**}}{R} = \delta_1^{**} = \delta_1\left(\frac{37}{315} - \frac{\lambda_1}{945} - \frac{\lambda_1^2}{9072}\right) - \delta_1^2\left(\frac{5}{126} - \frac{\lambda_1}{945} - \frac{\lambda_1^2}{30240}\right) - \Gamma_1\left(\frac{1}{45} + \frac{\lambda_1}{2160} + \frac{\Gamma_1}{240}\right). \tag{19}$$

Substitution of δ^* from (18) into (11) gives the relationship between the average and centre-line velocities as

$$\frac{U_0}{U_c} = 1 - \delta_1\left(\frac{3}{5} - \frac{\lambda_1}{60}\right) + \delta_1^2\left(\frac{2}{15} - \frac{\lambda_1}{180}\right) + \frac{\Gamma_1}{20}, \tag{20}$$

which restates that U_c should be read as U_∞ and $\Gamma_1 = 0$ in the inlet region.

Schlichting's (1968, p. 176) procedure was to use a continuity relation of the form of (20) with the right-hand side expressed as a series. This has been objected to by Van Dyke and Wilson because the resulting series for the potential-core velocity is not adequate to account for the boundary-layer effects. We propose to comply with the later suggestions by deriving a differential continuity equation from (11) and solving it simultaneously with the momentum equation (10), for δ and λ in the inlet region and for λ and Γ in the filled region. This will not require approximating the core velocity by an algebraic series.

The differentiated form of (11) is

$$(1 - 2\delta_1^*)\frac{dU_c}{dx} - 2U_c\frac{d\delta_1^*}{dx} = 0,$$

which by rearrangement and use of the definition of λ may be written for the inlet region as

$$d\delta_1^*/dx = \tfrac{1}{2}(1 - 2\delta_1^*)\,\nu\lambda/\delta^2 U_\infty. \tag{21}$$

Substitution of $\delta \equiv R$ and $U_\infty \equiv U_c$ make the equation applicable for the filled region.

The wall skin-friction coefficient C_f can be evaluated from the velocity profile (15) as

$$\frac{C_f}{2} = \frac{\tau_w}{\rho U_\infty^2} \equiv \frac{\tau_w}{\rho U_c^2} = \frac{\mu[\partial u/\partial y]_{y=0}}{\rho U_c^2} = \frac{\nu(2 + \frac{1}{6}\lambda_1 - \Gamma_1)\,U_c}{\delta U_c^2}, \tag{22}$$

which results in

$$C_f\frac{Re}{4} = \frac{1}{\delta_1}\left[2 + \frac{\lambda_1}{6} - \Gamma_1\right]\frac{U_0}{U_c}, \tag{23}$$

where $Re = U_0 D/\nu$.

3.2. *Solution of the governing equation*

The expressions (18), (19) and (23) for δ^*, δ^{**} and C_f can now be substituted into the integrated momentum equation (10) and the differentiated continuity (21) to yield a pair of ordinary differential equations for δ_1 and λ_1 in the inlet region and for λ_1 and Γ_1 in the filled region.

In the inlet region $\Gamma_1 = 0$, and the resulting simultaneous differential equations are

$$\frac{d\delta_1}{d\xi} = \frac{(U_0/U_\infty)\,[\delta_1 F_1(\lambda_1, \delta_1) - \lambda_1 F_2(\lambda_1, \delta_1)]}{\delta_1^2 F_3(\lambda_1, \delta_1)} \tag{24}$$

and

$$\frac{d\lambda_1}{d\xi} = \frac{1}{F_6(\lambda_1, \delta_1)}\left[\delta_1^2 F_4(\lambda_1, \delta_1)\frac{d\delta_1}{d\xi} - F_5(\lambda_1, \delta_1)\left(\frac{U_0}{U_\infty}\right)^2\right], \tag{25}$$

where $\xi = x/R\,Re$.

In the filled region $\delta_1 = 1$, and the corresponding equations are

$$\frac{d\lambda_1}{d\xi} = -30(7\lambda_1 + 12)\left(\frac{U_0}{U_c}\right)^2 - \frac{9}{2}\frac{d\Gamma_1}{d\xi} \tag{26}$$

and

$$\frac{d\Gamma_1}{d\xi} = \frac{U_0}{U_c}\frac{F_7(\lambda_1, \Gamma_1)}{F_8(\lambda_1, \Gamma_1)}. \tag{27}$$

The functions F_i are defined in the appendix. The above two pairs of equations, (24) and (25), and (26) and (27), are solved successively for the inlet and the filled regions by the fourth-order Runge–Kutta method.

The boundary layer is assumed to grow from the inlet of the pipe, requiring $\delta_1 = 0$ at $\xi = 0$. This condition further requires that $\lambda = 0$ at $\xi = 0$, so that (25) is also satisfied at the inlet of the pipe. For numerical solution, starting values of $\xi = 10^{-4}$, $\delta_1 = 2 \times 10^{-2}$ and $\lambda_1 = 0{\cdot}015$ with increments in ξ of 10^{-8} have been found to be suitable and to be invariant under small changes in the initial values of δ_1 and λ_1.

The solution for the inlet region is continued till δ_1 becomes equal to 1, i.e. up to the point where the boundary layers meet at the pipe centre. This takes place at $\xi = 0{\cdot}036$, where $\lambda_1 = 2{\cdot}7270$.

The solution for the filled region has been obtained with an initial value of λ_1 equal to the value at the end of the inlet region, $\delta_1 = 1{\cdot}0$. Here the value of Γ_1 is still zero and hence this is the starting value for the filled region.

It was pointed out that the fully developed profile is reached where $\lambda_1 = -\frac{12}{7}$ and $\Gamma_1 = -\frac{2}{7}$. Ideally, therefore, the end of the filled region should be marked by the attainment of these values of λ_1 and Γ_1. As would be expected, however, the approach to these values in the numerical calculation was extremely gradual and the practical limit of the filled region was chosen as the point where the average velocity corresponded to 99 % of the fully developed value. The 99 % limit was reached at $\xi = 0{\cdot}150$, where the numerically attained values of λ_1 and Γ_1 were $-1{\cdot}6831$ and $-0{\cdot}2839$, deviating respectively by less than 2 and 0·5 % from their exact values of $-1{\cdot}7143$ ($\lambda_1 = -\frac{12}{7}$) and $-0{\cdot}2857$ ($\Gamma_1 = -\frac{2}{7}$). The velocity profile, shear stress and pressure at a point were then evaluated using the estimated values of δ_1, λ_1 and Γ_1.

3.3. *Pressure drop*

In the inlet region there always exists a potential core; hence the pressure drop is estimated from Bernoulli's equation

$$\frac{p_0}{\rho} + \tfrac{1}{2}U_0^2 = \frac{p}{\rho} + \tfrac{1}{2}U_\infty^2,$$

or

$$\frac{p_0 - p}{\frac{1}{2}\rho U_0^2} = \left(\frac{U_\infty}{U_0}\right)^2 - 1 = \left(\frac{1}{1 - 2\delta_1^*}\right)^2 - 1. \tag{28}$$

In the filled region, in which there is no potential core, stepwise integration of the pressure gradient equation (6), using a Taylor series, is carried out.

In non-dimensional form the equation for $\delta_1 = 1$ is

$$dp^*/d\xi = -\tfrac{2}{3}(12 + 7\lambda_1 - 84\Gamma_1)\, U_c/U_0, \tag{29}$$

where $p^* = p/\frac{1}{2}\rho U_0^2$. The beginning of the filled region $\Gamma_1 = 0$ also belongs to the inlet region, and the initial value of $dp^*/d\xi$ is

$$dp^*/d\xi = -\tfrac{2}{3}(12 + 7\lambda_1)\, U_c/U_0. \tag{30}$$

The calculated values of ξ, the velocity ratio U_∞/U_0 or U_c/U_0, the skin-friction coefficients C_f and C_{f1} ($= \tau_w/\frac{1}{2}\rho U_0^2$), the non-dimensional parameters δ_1, Γ_1 and λ_1 and the pressure drop along the pipe in the inlet and filled regions are given in tables 1 and 2 respectively. The pressure-drop values estimated by Schiller and by Atkinson & Goldstein (see Goldstein 1938) are also given for comparison.

ξ	$\frac{U_\infty}{U_0}$	$\frac{1}{4}C_f Re$	$\frac{1}{4}C_{f1} Re$	δ_1	λ_1	$\frac{p_0-p}{\frac{1}{2}\rho U_0^2}$ (present)	$\frac{p_0-p}{\frac{1}{2}\rho U_0^2}$ (Schiller)	$\frac{p_0-p}{\frac{1}{2}\rho U_0^2}$ (Atkinson & Goldstein)
0·0010	1·1354	8·9680	11·5620	0·2157	1·1780	0·2892	0·32	—
0·0040	1·2700	4·4220	7·1320	0·4089	1·7770	0·6128	0·65	—
0·0080	1·3761	3·1110	5·8910	0·5481	2·0770	0·8935	—	—
0·0121	1·4580	2·5110	5·3375	0·6489	2·2520	1·1260	—	—
0·0151	1·5089	2·2340	5·0861	0·7091	2·3450	1·2770	1·33	1·36
0·0201	1·5834	1·9170	4·8063	0·7943	2·4660	1·5070	—	1·63
0·0251	1·6490	1·6980	4·6170	0·8667	2·5610	1·7190	—	1·88
0·0301	1·7082	1·5350	4·4790	0·9305	2·6420	1·9180	—	2·10
0·0331	1·7414	1·4550	4·4120	0·9657	2·6860	2·0330	—	—
0·0361	1·7742	1·3850	4·3600	1·0000	2·7270	2·1440	—	—

TABLE 1. Inlet region.

ξ	$\frac{U_c}{U_0}$	$\frac{1}{4}C_f Re$	$\frac{1}{4}C_{f1} Re$	λ_1	Γ_1	$\frac{p_0-p}{\frac{1}{2}\rho U_0^2}$	$\frac{p_0-p}{\frac{1}{2}\rho U_0^2}$ (Schiller)	$\frac{p_0-p}{\frac{1}{2}\rho U_0^2}$ (Atkinson & Goldstein)
0·0361	1·7742	1·3850	4·3600	2·7270	0·0000	2·1440	—	—
0·0400	1·8112	1·3210	4·3330	1·9780	−0·0635	2·2900	—	2·51
0·0500	1·8794	1·1950	4·2210	0·5695	−0·1518	2·6590	—	2·88
0·0600	1·9221	1·1220	4·1450	−0·2706	−0·2014	3·0120	—	3·24
0·0700	1·9493	1·0780	4·0960	−0·7874	−0·2316	3·3530	—	3·50
0·0800	1·9668	1·0500	4·0620	−1·1130	−0·2507	3·6870	—	3·93
0·0900	1·9782	1·0400	4·0449	−1·3220	−0·2629	4·0160	—	4·26
0·0923	1·9803	1·0320	4·0390	−1·3590	−0·2650	4·0910	—	—
0·1000	1·9860	1·0210	4·0260	−1·4580	−0·2708	4·3420	—	4·59
0·1100	1·9906	1·0140	4·0180	−1·5460	−0·2759	4·6660	—	4·92
0·1200	1·9938	1·0090	4·0110	−1·6030	−0·2793	4·9890	—	—
0·1300	1·9959	1·0060	4·0075	−1·6410	−0·2815	5·3100	—	—
0·1400	1·9973	1·0040	4·0050	−1·6660	−0·2829	5·6310	—	—
0·1500	1·9982	1·0030	4·0050	−1·6830	−0·2839	5·9520	—	—
				Exact (−1·7143)	(−0·2857)			

TABLE 2. Filled region ($\delta_1 = 1$).

4. Experiments

Experimental verification of the existence of inlet and filled regions and the measurement of the associated parameters were carried out in laminar incompressible flow of air through a 30 mm I.D. smooth aluminium pipe at three Reynolds numbers (1875, 2500 and 3250). The uniform velocity at entry was created by preceding the pipe with a short smooth bellmouth at the end of a large settling chamber. Fine wire-mesh screens were put inside the settling chamber, the area of which was more than 100 times larger than the pipe cross-section, resulting in near-stagnation conditions in the chamber. The connexion between the short bellmouth of the settling chamber and the aluminium pipe was made of a resin bonding (Araldite) and hand polished for smoothness. The inside of the aluminium pipe was also polished with grinding paste. The entire set-up was held rigidly, and with these precautions the flow in the entrance region, according to pressure-gradient values, was laminar even when the Reynolds number was marginally higher (2500 or 3250) than the standard or fully developed critical value.

The velocity field traverse was carried out by means of a 2 mm microprobe flattened at the tip, in conjunction with an Askania micromanometer of sensitivity 0·01 mm Hg. The accuracy of measurements was estimated to be better than 95 % by making calibration measurements in the fully developed flow region of the pipe.

5. Results and discussions

The laminar incompressible flow in the entrance region of a smooth pipe has been analysed on the basis of the existence of two distinct regions, the inlet and filled regions.

Fourth-degree velocity profiles with pressure-gradient parameters λ in the inlet region, and λ and Γ in the filled region were used to solve simultaneously the continuity and momentum equations by Pohlhausen's integral method, and the variation of δ, λ and Γ was predicted. The continuity equation used for numerical solution was in the form of a differential equation for the displacement thickness; thus there was no necessity to approximate the core velocity by an algebraic series or other form.

The acceleration of the potential core is reflected in the positive and increasing value of λ_1 in the inlet region, and such acceleration is destroyed in the filled region by the existence of a negative Γ_1; the numerically calculated terminal values of λ_1 and Γ_1 at the end of the entrance region deviate from the exact values by less than 2 and 0·5 %, respectively, and lend credibility to the accuracy of the solution. The exact variation of λ_1 and Γ_1 is tabulated in tables 1 and 2 and is also given in figures 2 and 3. The end of the entrance length corresponds to the attainment of 99 % of the average velocity of the Poiseuille flow.

The development of the boundary layer in the inlet region, which was estimated numerically and verified experimentally, is shown in figure 4. The end of the inlet region occurs when δ becomes equal to R, at the location $\xi = x/(R\,Re) = 0{\cdot}036$. The boundary-layer thickness obtained from Schiller's profile was also calculated and is presented in the same figure for comparison.

The numerically estimated values of the wall skin-friction coefficients C_f, based on the centre-line velocity, and C_{f1} based on the average velocity, were attained almost exactly (figure 5); as $\frac{1}{4}C_f\,Re = 1{\cdot}0$ and $\frac{1}{4}C_{f1}\,Re = 4{\cdot}0$ at the end of the entrance region

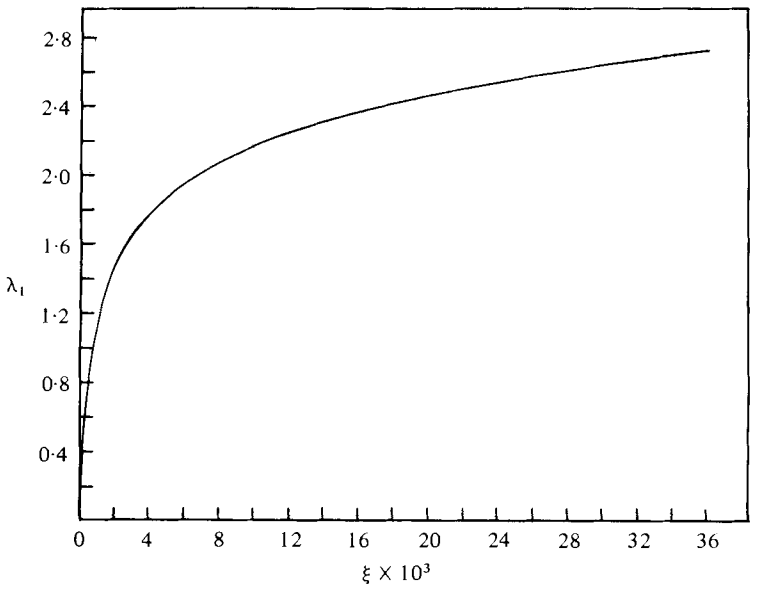

FIGURE 2. Pressure-gradient parameter λ_1 in the inlet region.

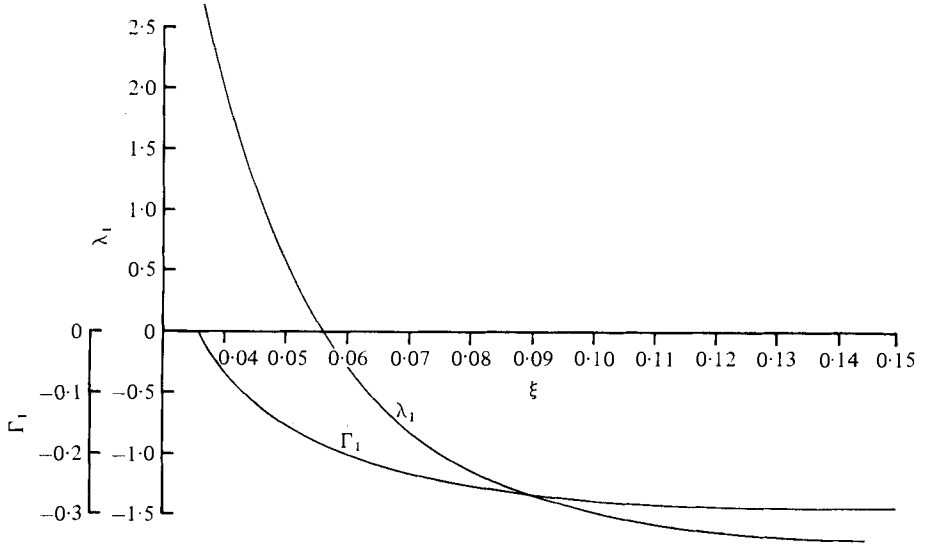

FIGURE 3. Pressure-gradient parameters in the filled region.

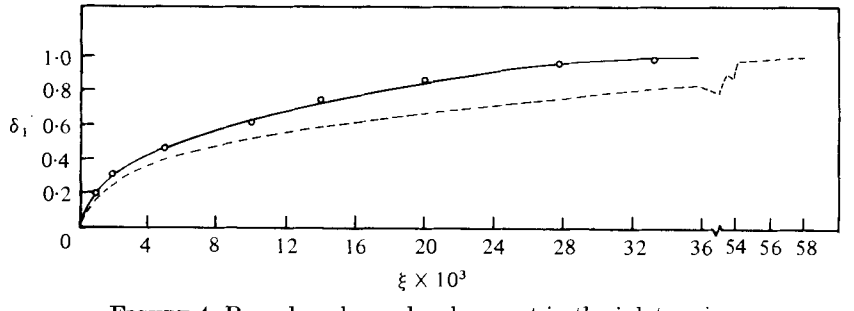

FIGURE 4. Boundary-layer development in the inlet region. ——, theory; —o—, experiment; - - - -, Schiller's theory.

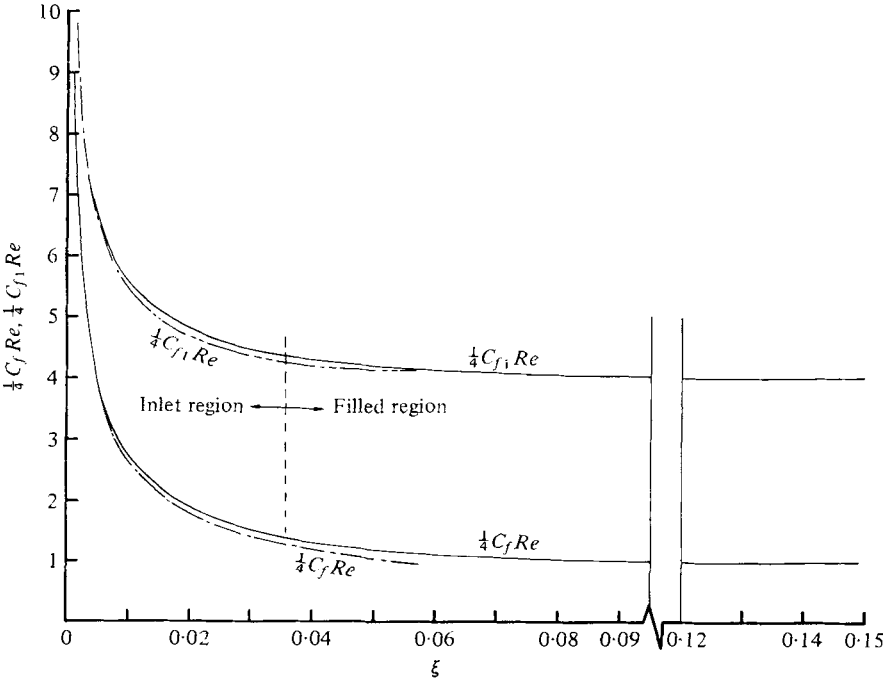

FIGURE 5. Skin-friction coefficients in the entrance region. ——, present investigation; —·—, — - - -, Schiller's theory. $C_f = \tau_w/\frac{1}{2}\rho U_\infty^2, C_{f1} = \tau_w/\frac{1}{2}\rho U_0^2, Re = 2U_0 R/\nu, U_0$ = average velocity.

($\xi = 0{\cdot}150$). Such a value of the entrance length is comparable with the results of Campbell & Slattery (1963, $\xi = 0{\cdot}136$), Atkinson & Goldstein (see Goldstein, 1938, $\xi = 0{\cdot}130$), Hornbeck (1964, $\xi = 0{\cdot}114$) and Gupta (1977), who followed the method of Campbell & Slattery, except for a modification in evaluating the shear stress, and obtained practically the same results as Campbell & Slattery. Similarly, the present value of $\xi = 0{\cdot}15$ is in good agreement with the measurements of Fargie & Martin (1971), who indicated attainment of a fully developed centre-line velocity at about $\xi = 0{\cdot}13$, for $760 < Re < 1512$. As the present results are based on boundary-layer analysis, they are unlikely to be accurate for low Reynolds numbers, say below 500.

The equations in both the inlet and the filled region are of boundary-layer form; thus it would be expected that the axial pressure gradient estimated with or without recognition of the existence of the two separate regions should be in good agreement. This is noted in tables 1 and 2 and in figure 6, where experimental results from the present investigation are also indicated. It may be noted that the present estimated value of the pressure at the end of the entrance region is closer to the Poiseuille value than any hitherto published.

The calculated values of the velocity profiles at different axial locations also agree well with experimental results briefly reported elsewhere (Mohanty & Asthana 1977), but are not presented here for brevity, the primary objective of the paper being to make a quantitative estimation of the lengths of the inlet and filled regions, which together constitute the entrance length.

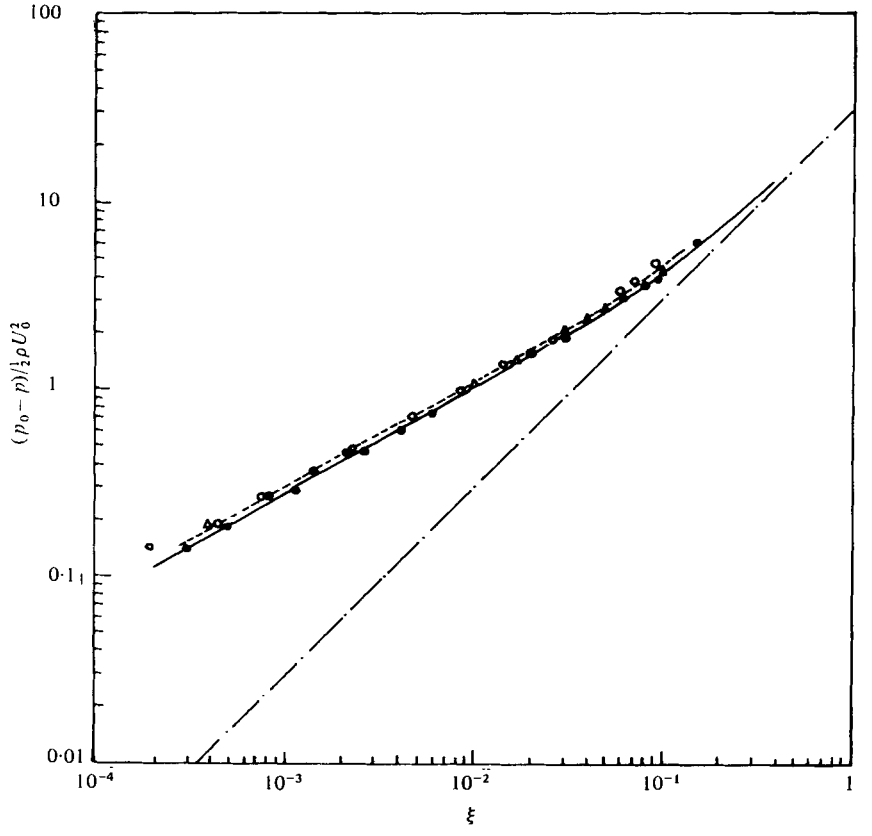

FIGURE 6. Entrance-region pressure drop. —·—, Poiseuille flow; – – –, Schiller (1922); △, Langhaar (1942); ○, Campbell & Slattery (1963); ——, present theory; ●, present experiments.

Appendix

$$F_1(\lambda_1,\delta_1) = (118-\tfrac{5}{3}\lambda_1)-\delta_1(\tfrac{483}{5}-\tfrac{113}{60}\lambda_1)+\delta_1^2(35-\tfrac{7}{5}\lambda_1)-\delta_1^3(\tfrac{76}{15}-\tfrac{41}{180}\lambda_1),$$

$$F_2(\lambda_1,\delta_1) = (4+\tfrac{5}{6}\lambda_1)+\delta_1(\tfrac{262}{15}-\tfrac{433}{360}\lambda_1)-\delta_1^2(\tfrac{567}{60}-\tfrac{343}{720}\lambda_1) -\delta_1^3(\tfrac{69}{180}-\tfrac{1}{360}\lambda_1)+\delta_1^4(\tfrac{19}{45}-\tfrac{41}{2160}\lambda_1),$$

$$F_3(\lambda_1,\delta_1) = (\tfrac{537}{200}-\tfrac{1}{4}\lambda_1+\tfrac{1}{288}\lambda_1^2)-\delta_1(2-\tfrac{5}{24}\lambda_1+\tfrac{1}{288}\lambda_1^2)+\delta_1^2(\tfrac{3}{10}-\tfrac{1}{30}\lambda_1+\tfrac{1}{1440}\lambda_1^2),$$

$$F_4(\lambda_1,\delta_1) = (108-3\lambda_1)-\delta_1(48-2\lambda_1),$$

$$F_5(\lambda_1,\delta_1) = (720\delta_1+360\lambda_1+60\lambda_1\delta_1),$$

$$F_6(\lambda_1,\delta_1) = \delta_1^3(3-\delta_1),$$

$$F_7(\lambda_1,\Gamma_1) = -95040+22608\lambda_1+168\lambda_1^2-473904\Gamma_1 -4248\lambda_1\Gamma_1-972\Gamma_1^2+21\lambda_1^2\Gamma_1-567\lambda_1\Gamma_1^2,$$

$$F_8(\lambda_1,\Gamma_1) = 864-9\lambda_1+243\Gamma_1.$$

REFERENCES

CAMPBELL, W. D. & SLATTERY, J. C. 1963 *Trans. A.S.M.E., J. Basic Engng* D **85**, 41.

FARGIE, D. & MARTIN, B. W. 1971 *Proc. Roy. Soc.* A **321**, 461.

GOLDSTEIN, S. 1938 *Modern Developments in Fluid Dynamics*. Oxford University Press.

GUPTA, R. C. 1977 *Appl. Sci. Res.* **33**, 1.

HORNBECK, R. W. 1964 *Appl. Sci. Res.* A **13**, 224.

LANGHAAR, H. L. 1942 *Trans. A.S.M.E., J. Appl. Mech.* A **64**, 55.

MCCOMAS, S. T. 1967 *Trans. A.S.M.E., J. Basic Engng* D **89**, 847.

MOHANTY, A. K. & ASTHANA, S. B. L. 1977 *6th Austral. Hydraul. Fluid Mech. Conf., Adelaide*, p. 532.

ROSENHEAD, L. 1963 *Laminar Boundary Layers*. Oxford University Press.

SCHLICHTING, H. 1968 *Boundary Layer Theory*. McGraw-Hill.

SHINGO, I. 1966 *Bull. Japan Soc. Mech. Engrs* **9**, 86.

SPARROW, E. M. & ANDERSON, C. E. 1977 *Trans. A.S.M.E., J. Fluids Engng* **99**, 556.

VAN DYKE, M. D. 1970 *J. Fluid Mech.* **44**, 813.

WHITE, F. M. 1974 *Viscous Fluid Flow*. McGraw-Hill.

WILSON, S. D. R. 1971 *J. Fluid Mech.* **46**, 787.